NeuroImage 179 (2018) 570–581

Contents lists available at ScienceDirect

NeuroImage

journal homepage: www.elsevier.com/locate/neuroimage

Scale-invariant rearrangement of resting state networks in the human brain under sustained stimulation

Silvia Tommasin [a,b,1], Daniele Mascali [a,1], Marta Moraschi [a], Tommaso Gili [a,c], Ibrahim Eid Hassan [d], Michela Fratini [c,e], Mauro DiNuzzo [f], Richard G. Wise [g], Silvia Mangia [h], Emiliano Macaluso [i], Federico Giove [a,c,*]

[a] Centro Fermi - Museo storico della fisica e Centro di studi e ricerche Enrico Fermi, Roma, Italy
[b] Dipartimento di Neuroscienze umane, Sapienza Università di Roma, Roma, Italy
[c] Fondazione Santa Lucia IRCCS, Roma, Italy
[d] Department of Physics, Helwan University, Cairo, Egypt
[e] Istituto di Nanotecnologia, Consiglio Nazionale delle Ricerche, Roma, Italy
[f] Center for Basic and Translational Neuroscience, Faculty of Health and Medical Sciences, University of Copenhagen, Copenhagen, Denmark
[g] Cardiff University Brain Research Imaging Centre (CUBRIC), School of Psychology, Cardiff University, Cardiff, UK
[h] Center for Magnetic Resonance Research, Dept. of Radiology, University of Minnesota, Minneapolis, USA
[i] ImpAct Team, Lyon Neuroscience Research Center, Lyon, France

ARTICLE INFO

Keywords:
Functional connectivity
Steady-state networks
Working memory
Connectivity dynamics

ABSTRACT

Brain activity at rest is characterized by widely distributed and spatially specific patterns of synchronized low-frequency blood-oxygenation level-dependent (BOLD) fluctuations, which correspond to physiologically relevant brain networks. This network behaviour is known to persist also during task execution, yet the details underlying task-associated modulations of within- and between-network connectivity are largely unknown. In this study we exploited a multi-parametric and multi-scale approach to investigate how low-frequency fluctuations adapt to a sustained n-back working memory task. We found that the transition from the resting state to the task state involves a behaviourally relevant and scale-invariant modulation of synchronization patterns within both task-positive and default mode networks. Specifically, decreases of connectivity within networks are accompanied by increases of connectivity between networks. In spite of large and widespread changes of connectivity strength, the overall topology of brain networks is remarkably preserved. We show that these findings are strongly influenced by connectivity at rest, suggesting that the absolute change of connectivity (i.e., disregarding the baseline) may not be the most suitable metric to study dynamic modulations of functional connectivity. Our results indicate that a task can evoke scale-invariant, distributed changes of BOLD fluctuations, further confirming that low frequency BOLD oscillations show a specialized response and are tightly bound to task-evoked activation.

1. Introduction

Spatially correlated, low-frequency BOLD oscillations occur in the brain both at rest and during the execution of a task (Rogers et al., 2007). The physiological relevance of low-frequency brain fluctuations during the resting state is evidenced by the existence of brain-wide networks that span across functionally-linked cortical areas (Damoiseaux et al., 2006; Yeo et al., 2011). Low-frequency BOLD fluctuations have been also shown to influence behaviour (Fox et al., 2007; Hampson et al., 2006) and contribute to variability in task-evoked responses (Fox et al., 2006). Noticeably, alterations of functional connectivity (FC) have been associated with several brain diseases (Calhoun et al., 2008; Gili et al., 2011; Greicius, 2008; Mascali et al., 2015, 2018; Prodoehl et al., 2014).

Considerable efforts have been devoted to characterize stationary task-related changes of brain networks, recently reviewed by Gonzalez-Castillo and Bandettini (2017). In general, multiple classes of evoked activity, while introducing task-specific features, do not significantly change the whole-brain patterns of correlated intrinsic fluctuations (Cole et al., 2014). Indeed, when subjects are cognitively engaged, correlated fluctuations seem to preserve their spatial structure (although with

* Corresponding author. Dipartimento di Fisica, Sapienza Università di Roma, Piazzale Aldo Moro, 5 00185, Roma, Italy.
E-mail address: federico.giove@uniroma1.it (F. Giove).
[1] These authors contributed equally to this work.

https://doi.org/10.1016/j.neuroimage.2018.06.006
Received 23 April 2018; Accepted 4 June 2018

intensity modulations) within both the default mode network (DMN) (Fransson, 2006; Vatansever et al., 2015b) and the task-positive network (Fox et al., 2005). Accordingly, Independent Component Analysis (ICA) decompositions of resting state and task-based fMRI response showed almost overlapping areas (Smith et al., 2009).

In spite of this consistency, the spatial scale and behavioural relevance of connectivity modulations associated with task executions are not yet completely understood. In fact, there is ambiguous evidence of how patterns of low frequency BOLD fluctuations change during the continuous performance of cognitive or sensory stimulations. Hampson et al. (2004) observed a spatial reduction of areas functionally connected to MT/V5 during a visual motion task, suggesting a transition to more spatially specialized network processes. On the other hand, other authors reported task-associated increments of functional connectivity between areas that are considered engaged during task-based experiments (Hampson et al., 2002; Lowe et al., 2000; Newton et al., 2007), but even in this case the phenomenon was explained in terms of a change of the connected subareas within a network (Newton et al., 2007). Within the DMN, task-associated reductions of connectivity have been usually observed (Gordon et al., 2014; Hampson et al., 2006), along with DMN deactivation (Fornito et al., 2012), and have thus been interpreted as evidence for DMN disengagement induced by task (see Anticevic et al., 2012 and references therein). Similar conclusions were drawn based on more complex behaviours of DMN connectivity, suggestive of an internal specialized structure, responding to the task with dissociation (Fornito et al., 2012; Leech et al., 2011). Converging evidence suggests that this internal dissociation might arise from the dynamic cooperation of DMN components with regions actively engaged by the task (Bray et al., 2015; Fornito et al., 2012; Leech et al., 2011; Piccoli et al., 2015; Spreng et al., 2010).

Connectivity within the DMN at rest and during task execution, but not the task-associated change of connectivity, were found to be correlated with performance in an n-back task, suggesting that DMN connectivity is a prerequisite for correct task execution (Hampson et al., 2006). Similarly, the connectivity between DMN and other networks during task execution has been repeatedly shown to be behaviourally relevant. Vatansever and colleagues (Vatansever et al., 2015b) reported that connectivity between DMN and somatomotor network during a motor task predicts faster motor reaction times. Fornito et al. (2012) found that connectivity between the DMN and selected areas of the task positive network is associated with more rapid memory recollection. Finally, Elton and Gao observed a significant relationship between flexible changes of DMN connectivity and behaviour, indicating the behavioural relevance not only of network features during task, but also of network changes associated with tasks covering multiple domains (Elton and Gao, 2015a, 2015b). In addition, Shultz and Cole reported that a smaller topological reorganization of whole-brain networks during task is related to behavioural performance and to personal intelligence (Schultz and Cole, 2016). This latter result is rather at odd with previous reports showing that a high degree of whole-brain fast network reconfiguration during n-back task is correlated to enhanced working memory performance and overall cognitive flexibility (Braun et al., 2015).

Albeit the heterogeneity of the experimental procedures renders any strict conclusion difficult, two issues are likely to be related to the previously described, somewhat incoherent findings: 1) the baseline upon which connectivity changes are computed and 2) the spatial scale at which the connectivity is probed. Regarding the former point, various relationships characterized by variable specificity have been found between pre-stimulus baseline and brain connectivity (Gordon et al., 2014; Tailby et al., 2015). Accordingly, it has been suggested that evoked activity may not be simply additive over baseline (Huang et al., 2017 and references therein). In addition, the ongoing debate around the suitability of global signal regression in resting-state analyses highlights the importance of defining a proper baseline (Murphy and Fox, 2017 and references therein). Regarding the latter point, conventional functional connectivity measures include also long range correlations, thus a multi-scale analysis including a strictly local measure of connectivity (e.g., regional homogeneity, Zang et al., 2004) can help disentangling the contribution from network modules of different size.

The aim of this study was to investigate the spatial scale at which functional connectivity is dynamically influenced by cognitive engagement, probing how connectivity changes in response to task execution. We also aimed at determining a suitable metric to identify behavioural relevant functional connectivity modulations. To this purpose, we extensively characterized network features during both resting state and sustained working memory (WM) task execution.

2. Material and methods

2.1. Subjects

Twenty right-handed Italian-speaking subjects (8 females, age 33 ± 6 years) participated in the study. All subjects were in good health and had no past history of neurological or psychiatric disease. Subjects had normal or corrected-to-normal (via contact lenses) visual acuity. The study was carried out in accordance with a protocol approved by the Ethics Committee of Santa Lucia Foundation in Rome. Recruited subjects gave written informed consent in accordance with the Declaration of Helsinki and European Union regulations.

2.2. Images acquisition

Data were collected on a 3 T MRI Scanner (Magnetom Allegra, Siemens Healthineers, Erlangen, Germany) equipped with a standard birdcage coil. Functional images were acquired via a Gradient-Echo Planar Imaging (GE-EPI) sequence (TR = 2100 ms, TE = 30 ms, FA = 70°, voxel size $3 \times 3 \times 2.5\ mm^3$) lasting 24 min and 38 s for a total of 704 volumes (4 dummy scans included). The slices were positioned starting from the vertex and covered the whole cerebrum. The cerebellum was not consistently included in the field of view of each subject, and was excluded from any analysis. High resolution T_1-weighted images were acquired for anatomic reference and tissue segmentation purpose using a Magnetization Prepared Rapid Acquisition Gradient Echo (MPRAGE, TE = 4.38 ms, TR = 2000 ms, FA = 8°, voxel size $1.33 \times 1.33 \times 1\ mm^3$).

2.3. Stimulation paradigm

The functional stimulation, composed of both auditory and visual components, was generated using Cogent 2000 (Laboratory of Neurobiology, Wellcome Trust, London, UK) under Matlab 7.1 (The Mathworks Inc., Natick, Massachusetts, USA) and delivered during functional scans through the standard MRI headphone system and through a digital light processing projector. The projector was located outside the magnet room and projected the visual stimulus on a screen positioned behind the subject, who viewed it through a mirror mounted on the head coil.

The stimulation paradigm (Supplementary Figure 1) consisted of alternated long-lasting epochs of open-eyes resting state and sustained auditory working memory task (4 min and 54 s each, starting with a resting-state epoch). The auditory working memory task involved continuous n-back trials administered in epochs either at “high” load (2-back) or “low” load (1-back). Each trial was composed of a 500-ms window, in which subjects were aurally presented with a vowel (pseudorandomly chosen among A, E, or O), and a subsequent 1600-ms response window, during which subjects had to report whether the current vowel was the same as the one presented one stimulus prior (1-back) or two stimuli prior (2-back). Subjects responded via an MRI compatible 2-button keyboard, with one button reserved for positive responses (matching trial) and one button reserved for negative responses (not matching trial). During the entire functional run, subjects were asked to maintain the gaze on the center of the screen which was marked by one degree circle over a uniform black background. The

fixation circle changed color to indicate the functional condition: grey for rest, red for vowel presentation window and green for response window. At the beginning of each working memory epoch the text "1-back" or "2-back" appeared on the screen. Subjects were trained for approximately 30 min before entering the scanner.

Two functional runs were acquired for each subject during the same experimental session, with epoch ordering: rest/1-back/rest/2-back/rest or rest/2-back/rest/1-back/rest. Run order was counterbalanced across subjects. The stimulation paradigm started after the second dummy scan (i.e., was overall shifted backwards by 2 TR) to roughly account for hemodynamic delay.

2.4. Working-memory performance

Subjects WM responses were monitored at runtime and recorded for later correlation analyses with FC metrics. Behavioural data from 3 subjects could not be recorded for technical problems, leaving a total of 17 subjects for behavioural analysis. Subject performance during each task epoch was evaluated in terms of accuracy obtained as the percentage of valid responses on the number of trials. A response was deemed valid if both correct and given during the response window.

2.5. Images preprocessing

Functional and structural MRI data were preprocessed using functional connectivity toolbox (CONN 17c; Whitfield-Gabrieli and Nieto-Castanon, 2012), and analysed with dedicated in-house routines based on Matlab R2013a (The Mathworks Inc., Natick, Massachusetts, USA) and AFNI (Cox, 1996). Preprocessing of functional data included the following steps: (i) removal of first four volumes (dummy scans) to assure that the MR signal reached stability (ii) compensation of systematic slice-dependent time shifts by phase shift in the Fourier domain, (iii) rigid body registration for inter-frame head motion within and across runs, (iv) unwarp algorithm to reduce the susceptibility-by-movements effects (Andersson et al., 2001) and (v) normalization to Montreal Neurological Institute (MNI) space (voxel size $2 \times 2 \times 2\,mm^3$) using as source image the EPI mean volume obtained from step ii. T_1 weighted images were segmented to obtain grey matter (GM), white matter (WhM) and cerebrospinal fluid (CSF) probability maps in MNI space. Any further analysis of functional data was constrained to a common GM mask which was defined by thresholding at 50% the across-subjects average of GM probability maps.

Functional data were further processed regressing out spurious variance using a general linear model (3dTproject, AFNI routine). The following regressors were included in the model: a second order Legendre polynomial, a basis of sines and cosines to model frequencies outside the band of interest (0.008–0.09 Hz), the six estimated motion parameters and their first derivative, the first five eigenvectors from time series within a WhM mask (obtained thresholding the subject probability map at 70% and eroding the resulting binary map by 2 voxels to avoid partial volume effects) and the first five eigenvectors from the time series within a CSF mask (threshold = 80%, one voxel erosion), following the aCompCor approach (Behzadi et al., 2007). To further reduce the impact of motion on BOLD time series, data were censored by removing time points with more than 0.4 mm of displacement (estimated as the Euclidian norm of motion parameters derivatives) along with each previous time point. The choice of the censoring threshold was not critical: preliminary testing showed that different thresholds did not impact the overall results. Censoring was applied during the regression step removing time points from both data and regressors. Finally, spatial smoothing, constrained to the common GM mask, was applied with an $8 \times 8 \times 8\,mm^3$ FWHM Gaussian kernel (3dBlurInMask, AFNI routine). An unsmoothed version of the data was retained for specific computation steps, as described below.

Each processed functional run was then split in its five epochs. The first resting state epoch of each run was used only for network definition and cortical parcellation, and then discarded from further processing to avoid double dipping (Kriegeskorte et al., 2009). The following four epochs were later used to extract epoch-related functional parameters.

2.6. Head motion assessment

The frame-wise displacement (FD), as defined in (Power et al., 2012), was computed to assess head movements during functional scans. For each run, the FD series obtained from the realignment parameters was split in 4 series corresponding to the 4 functional epochs. Then, the averaged FD was compared across epochs by paired t-tests.

2.7. ICA-based network definition

The first resting-state epochs of each run were analysed to extract the main resting-state networks which served as reference to study functional connectivity modulations associated with task execution. The networks were derived via group ICA using the FSL routine MELODIC (Beckmann and Smith, 2004). The decomposition was applied to the 4-dimensional time series obtained by concatenating in the temporal dimension the first resting-state epoch (of each run) of all studied subjects. Among the resulting eleven independent components we identified six networks of interest based on visual inspection and cross-correlation with the network atlas defined by Yeo et al. (2011). The six identified networks were labelled as Dorsal Attention (DAN), Default Mode (DMN), Frontoparietal (FPN), Somatomotor (SMN), Ventral Attention (VAN) and Visual (VIS) network (Fig. 1).

2.8. Cortical parcellation

To investigate functional connectivity modulations at multiple spatial scales, the cortex was parcelled into a variable number of ROIs, via a 2-level analysis that built group level ROIs based on the similarity between each voxel time courses. The approach, fully described elsewhere (Craddock et al., 2012), was applied to the same epochs used for ICA decomposition, and was used to obtain 150, 250, 350, 500, 750 and 1000 ROIs. ROIs were then classified into one of the ICA resting-state derived networks with a minimum overlap criterion (threshold = 65%). ROIs with insufficient overlap were excluded from further analyses, finally obtaining brain parcellations into 60, 110, 146, 227, 347, 477 ROIs, respectively.

2.9. Network metrics

The following metrics were computed to study task-associated

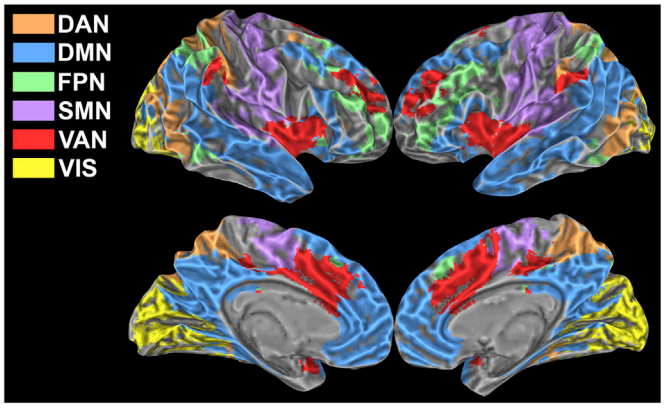

Fig. 1. Networks. Group networks identified via ICA applied to the first resting state epoch of each run. The six identified networks were labelled as Dorsal Attention (DAN), Default Mode (DMN), Frontoparietal (FPN), Somatomotor (SMN), Ventral Attention (VAN) and Visual (VIS) network.

modulations in network properties. Each metric was computed separately in each functional epoch, thus they represent specific network features at specific steady-state conditions. Prior to statistical comparison, metrics computed from homologous epochs belonging to different runs were averaged for each subject, after preliminary analyses that indicated a much lower variance between homologous epochs than between epochs corresponding to different conditions.

Within-network FC. For each ICA-derived network, we defined within-network FC as the average of z-Fisher transformed Pearson's coefficients obtained correlating each within-network voxel time-course with the network average time-course. To enhance signal-to-noise ratio without losing spatial specificity, the average network time course was extracted from unsmoothed functional data and correlated to smoothed data. The metric assesses the internal network coherence at large scale.

Between-network/ROIs FC. For each network (or ROI), an average time-course was extracted from unsmoothed data and correlated to each other network (or ROI) time-course, leading to a network-to-network (or ROI-to-ROI) correlation matrix. A z-Fisher transformation was applied to the correlation matrix to improve normality.

Regional Homogeneity. The similarity of time series at small spatial scale was evaluated by computing Regional Homogeneity (Zang et al., 2004). For each voxel in the common GM mask, ReHo was computed as the Kendall's coefficient of concordance among the selected voxel time series and the time series of its 18 nearest neighbours (3dReHo, AFNI). Given the known influence of spatial smoothing on ReHo (Xi-Nian Zuo et al., 2013), the computation was performed on unsmoothed data. ReHo values were then averaged in the ICA-derived networks to assess the internal network coherence at small scale (as opposed to within-network FC).

2.10. Statistical analyses

Task-associated changes of network metrics. Functional connectivity modulations associated with task execution were evaluated for statistical significance by repeated-measures ANOVA and paired t-tests. Tests were conducted for each functional metric (ReHo, within- and between-network FC) considering the following epochs: 1-back, rest, 2-back, rest. Prior to statistical comparison, the bias due to different amount of head movements during different steady-state epochs was mitigated by regressing out, via a general linear model, the epoch-averaged FD. ANOVA results were corrected for multiple comparisons (across networks) via false discovery rate (FDR).

Multi-scale assessment of task-associated changes in FC. For each parcellation scheme, the average correlation matrix at task (irrespectively of the cognitive load) was compared to the average correlation matrix at rest via paired t-tests. The epoch-averaged FD was used as nuisance covariate in statistical comparisons. For the 110-ROIs parcellation scheme, the significant task-associated changes in FC were assessed at $p < 0.05$, corrected via false discovery rate (FDR) using the Matlab toolbox NBS (https://www.nitrc.org/projects/nbs/), and their spatial representation was visualized with BrainNet Viewer (Xia et al., 2013).

Rest vs task FC relationship. To check for the influence of resting connectivity on connectivity changes, a linear model between FC at rest, FC_R, and FC at task FC_T, was tested:

$$FC_T = \beta_1 FC_R + \beta_0, \quad (1)$$

which implies for connectivity change $\Delta FC = FC_T - FC_R$ the following relationship:

$$\Delta FC = (\beta_1 - 1) FC_R + \beta_0 \quad (2)$$

The model in eq. (1) was tested separately for each subject using the 110-ROIs parcellation. Specifically, for each subject, correlation matrices calculated from resting epochs and those calculated from task epochs were averaged separately, leading to two correlation matrices. Then, the upper triangular part of the two correlation matrices were split according to the six ICA-derived networks, leading to 21 arrays of correlations which included 6 within-network and 15 between-network sets of correlations. For each array, correlations belonging to rest matrix FC_R and those belonging to task matrix FC_T were fed to the model in eq. (1). Finally, β_0 and β_1 were estimated via ordinary least squares method.

The explanatory power of linear and constant terms in eq. (2) were estimated by computing the respective coefficient of determination, R^2, as squared inter-subject Pearson's correlation coefficient between each of the two explanatory variable and ΔFC.

FC and subject's accuracy. The behavioural relevance of within and between-network FC was assessed via partial correlations with subject's accuracy in task execution, controlling for the effect of epoch-averaged FD. Accuracy was separately correlated with FC during rest, during task and with the relative change ($\Delta FC = FC_T - FC_R$). The behavioural relevance of the model in eq (1) was also tested correlating subject's accuracy with the estimated β_0 and β_1. Results were corrected for multiple comparisons via FDR.

Numerical results. All numerical results are given as mean ± standard deviation, unless otherwise stated.

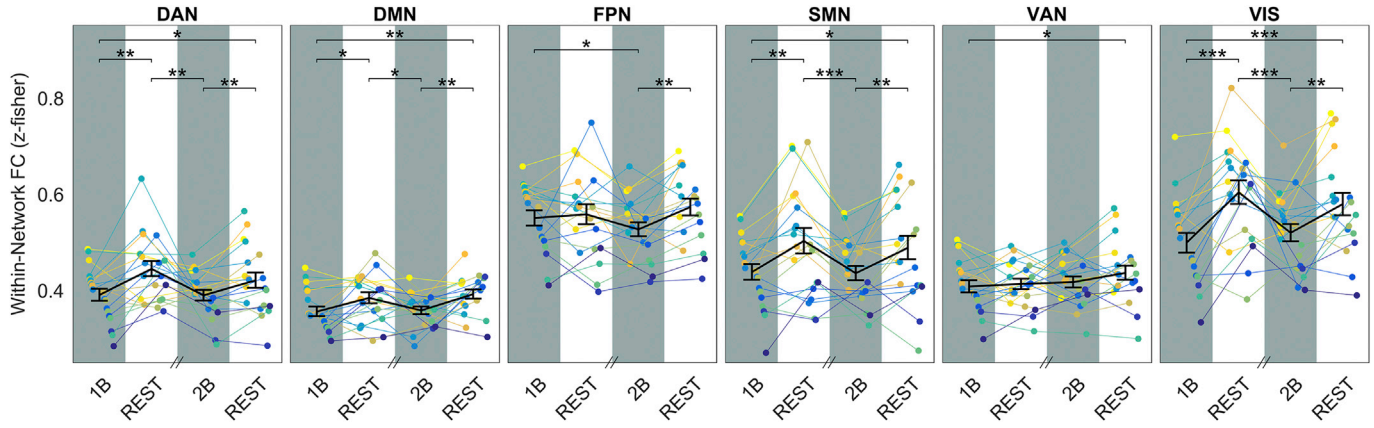

Fig. 2. Within-network FC across different steady-state epochs. Plots show the within-network FC for each ICA-derived network as a function of the epoch condition (1B, REST, 2B, REST). In each plot, the group-averaged mean and SEM are displayed on top of single subject time-courses. In 5 out of 6 networks, FC significantly differed among epochs (one-way repeated-measures ANOVA, FDR corrected: DAN, $p = 2.3*10^{-4}$; DMN, $p = 1.9*10^{-3}$; FPN, $p = 0.021$; SMN, $p = 1.4*10^{-4}$; VIS, $p = 2.2*10^{-6}$), being lower during task conditions compared to resting epochs as revealed by post-hoc paired t-tests. Significance of *t*-tests is marked with asterisks: *** $p < 0.001$, ** $p < 0.01$, * $p < 0.05$. Note than in this figure and in following Fig. 3 and 4 the horizontal axis does not represent a continuous timeline, because of randomization of epochs order (see Methods). However, each task epoch was kept together with the rest epoch immediately following it.

3. Results

3.1. Subjects' functional response and behaviour

Subjects' functional response to the complex task was strong and widespread, encompassing all the brain domains, and in particular all the investigated networks (Supplementary Figure 2).

Subjects' accuracy during task was consistently high and above chance level, with an average of (97 ± 2) % of correct responses during the low-load condition and (84 ± 8) % during the high-load condition. The two conditions significantly differed in subject's accuracy (paired *t*-test, $p < 10^{-5}$). Percentage of correct responses did not show any tendency to change during the second run (paired *t*-test, $p > 0.57$). As expected from previous studies (Huijbers et al., 2017), subjects moved more during resting epochs compared to task epochs, with an average FD of (0.14 ± 0.05) mm during rest and (0.09 ± 0.03) mm during task (paired *t*-test, $p < 10^{-5}$). To reduce the bias due to the different amount of head movements, results were corrected for the epoch-averaged FD.

3.2. Connectivity changes in the ICA-derived networks

The WM task influenced the synchronization of BOLD low-frequency fluctuations, leading to a diffused decrease of within-network functional connectivity compared with rest. Indeed, within-network FC was generally reduced during both low- and high-load task in all considered networks, including the DMN, with an average decrement of (7.8 ± 1.8) % (mean ± SEM, standard error of the mean) during task execution (Fig. 2). Increased cognitive load caused a significant effect only within FPN, with a reduction of connectivity at n = 2 vs n = 1 (p = 0.038).

The strong modulation of within-network connectivity was mirrored by widespread, opposite changes of between-network connectivity. The effect was very strong for DMN-VAN and DMN-DAN connectivity, and was well noticeable also in connections between DAN, VAN and FPN, namely DAN-VAN, DAN-FPN, VAN-FPN. All the between-network connections showed some significant task-related changes, except DMN-FPN, DMN-VIS and SMN-VAN. The detail of changes is shown in Fig. 3.

The behaviour of low-frequency fluctuations was essentially the same at the opposite extremum of the spatial scale we investigated,

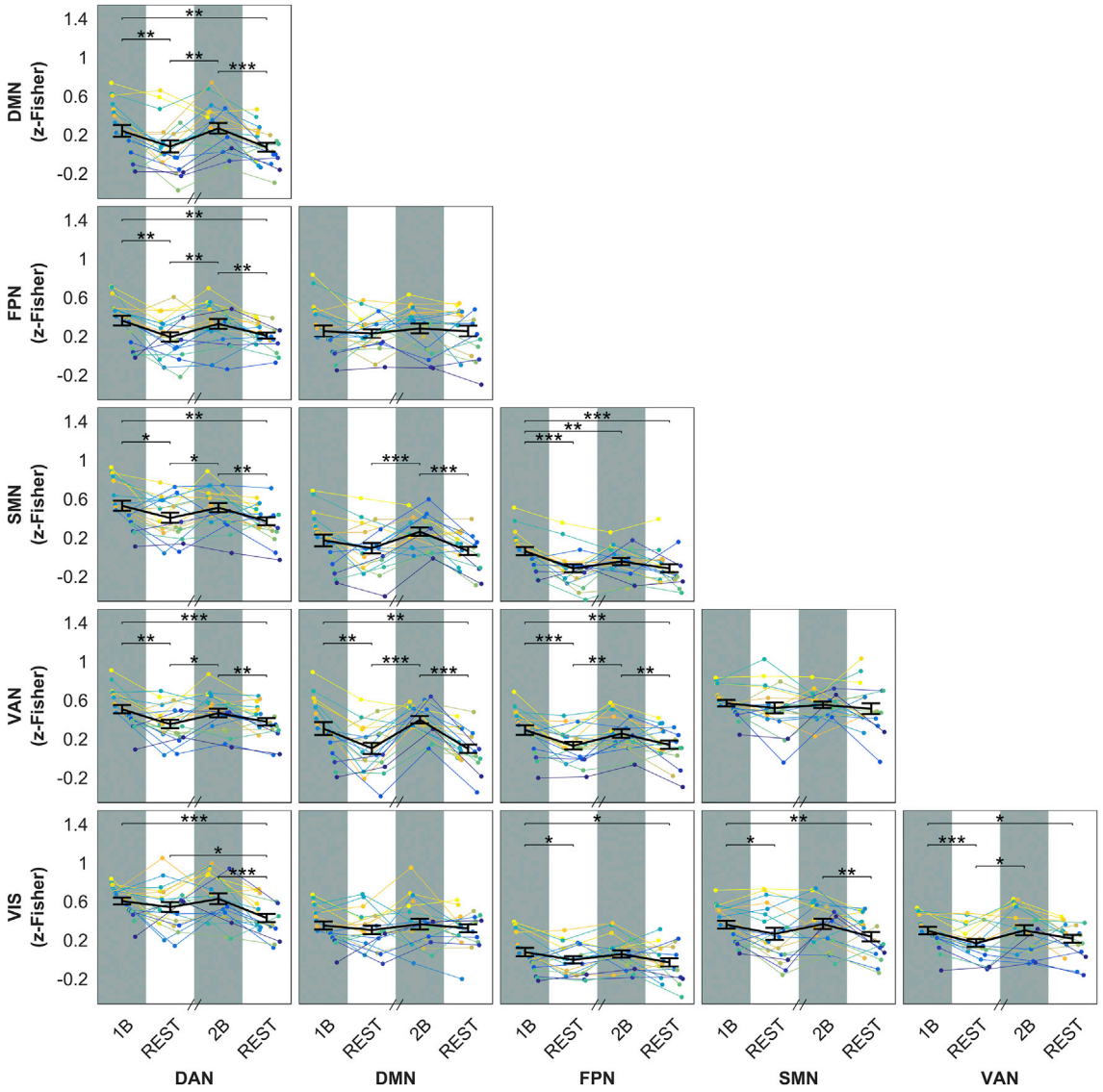

Fig. 3. Between-network FC across different steady-state epochs. Plots show the between-network FC for each ICA-derived network as a function of the epoch condition (1B, REST, 2B, REST). In each plot, the group-averaged mean and SEM are displayed on top of single subject time-courses. With the exception of three network pairs (DMN-FPN, DMN-VIS and VAN-SMN), each couple of networks showed significant differences in FC among epochs (one-way repeated-measures ANOVA, *p*-FDR < 0.05). Post-hoc paired *t*-tests showed significant increases in FC during task epochs (*** $p < 0.001$, ** $p < 0.01$, * $p < 0.05$).

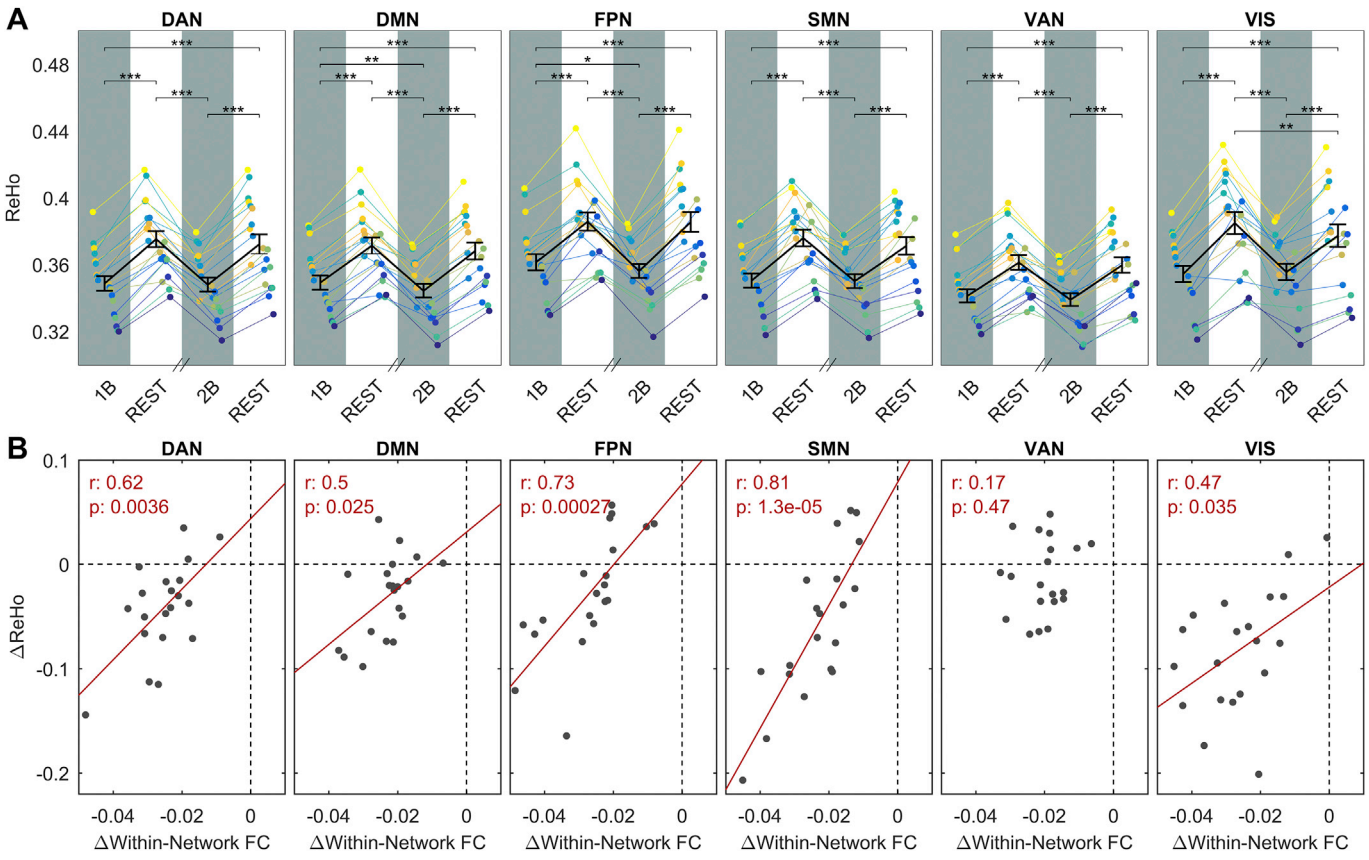

Fig. 4. A) ReHo across different steady-state epochs. Plots show ReHo values averaged in the six ICA-derived networks as a function of the epoch condition (1B, REST, 2B, REST). In each plot, the group-averaged mean and SEM are displayed on top of single subject time-courses. In all networks, ReHo significantly differed among epochs (one-way repeated-measures ANOVA, *p*-FDR « 10^{-5}) and was reduced by task, as revealed by post-hoc paired t-tests. Significance of *t*-tests is marked with asterisks: *** $p < 0.001$, ** $p < 0.01$, * $p < 0.05$. In DMN and FPN the reduction was characterized by a significant effect of load. **B) Correlations between ReHo changes and FC changes.** Correlation coefficient and p values were reported for each network. The correlation was significant for 5 out of 6 investigated networks.

represented by ReHo, which probes similarity among timeseries of neighbouring voxels. ReHo values averaged in the ICA-derived networks were systematically and substantially reduced during task by (6.4 ± 0.2) % (mean ± SEM). The effect was rather homogeneous in all networks, and within DMN and FPN was characterized by a significant effect of load (Fig. 4A). ReHo changes were correlated to changes of within-network connectivity in 5 out of 6 investigated networks, suggesting that the reported change of connectivity tends to be scale invariant within large brain networks (Fig. 4B).

3.3. Multi-scale assessment of connectivity changes

The multi-scale analysis showed an overall task-associated reduction in connectivity within each network (see the diagonal partitions in Fig. 5A and B), at each parcellation scale (from 60 to 477 ROIs), and thus at each ROI size (from 688 ± 181 to 108 ± 34 voxels). Connectivity between ROIs belonging to different networks was generally lower than connectivity between ROIs from the same network both at rest and at task, and had a tendency to increase during task (out of diagonal partitions in Fig. 5A and B). Internal structure of the DMN, showing anterior and posterior partitions characterized by a high internal integration and a weaker but discernible correlation between them, is seen at each parcellation scheme. The same feature emerged also for VAN, but limited to parcellations into high number of ROIs (from 146).

The spatial representation of significant changes of the adjacency matrix for 110-ROIs confirms that during task several internetwork connections increased their strength, including connectivity between nodes in the posterior DMN (cingulum) and motor areas (superior temporal gyrus), in DMN (parietal Inferior lobe) and DAN areas (middle occipital lobe), in DMN (superior frontal orbital gyrus) and VAN (temporal middle gyrus) areas, as well as connections between VIS areas (cuneus) and nodes in the supplementary motor area. In addition, significant higher connections were found between nodes in DAN and nodes in VAN and FPN (Fig. 6a). On the other hand, the decrease of connectivity related to task was mainly confined to nodes within the same network, with the DMN and especially its temporal areas representing the large majority of changes. Two exceptions, significant for amplitude of connectivity change and for their high degree of centrality, are a node in the precuneus (DAN), which strongly decreased its connectivity with nodes in the anterior and posterior DMN and in the FPN, and a node in the inferior frontal gyrus (FPN) that decreased its connectivity with a node in the anterior DMN.

3.4. Relationship between rest and task connectivity

In spite of the widespread task-related modulations of functional connectivity, the overall topology of brain networks was remarkably preserved in the transition from rest to WM task. Across the 110-ROIs parcellation, connectivity during task was highly correlated to connectivity at rest in the whole brain (Fig. 7A, $r = 0.94$, $p << 10^{-5}$). Similarity between networks at rest and during task was equally high within each of the investigated networks separately (Fig. 7B), and was only marginally reduced between ROIs in different networks (Fig. 7C), thus confirming the preservation of connectivity both within and between networks. Variability between subjects is represented in Supplementary figure 3, which shows the regression plots corresponding to Fig. 7B and C performed separately for each subject. Similarity between networks at rest and during task was conspicuously confirmed at each spatial scale

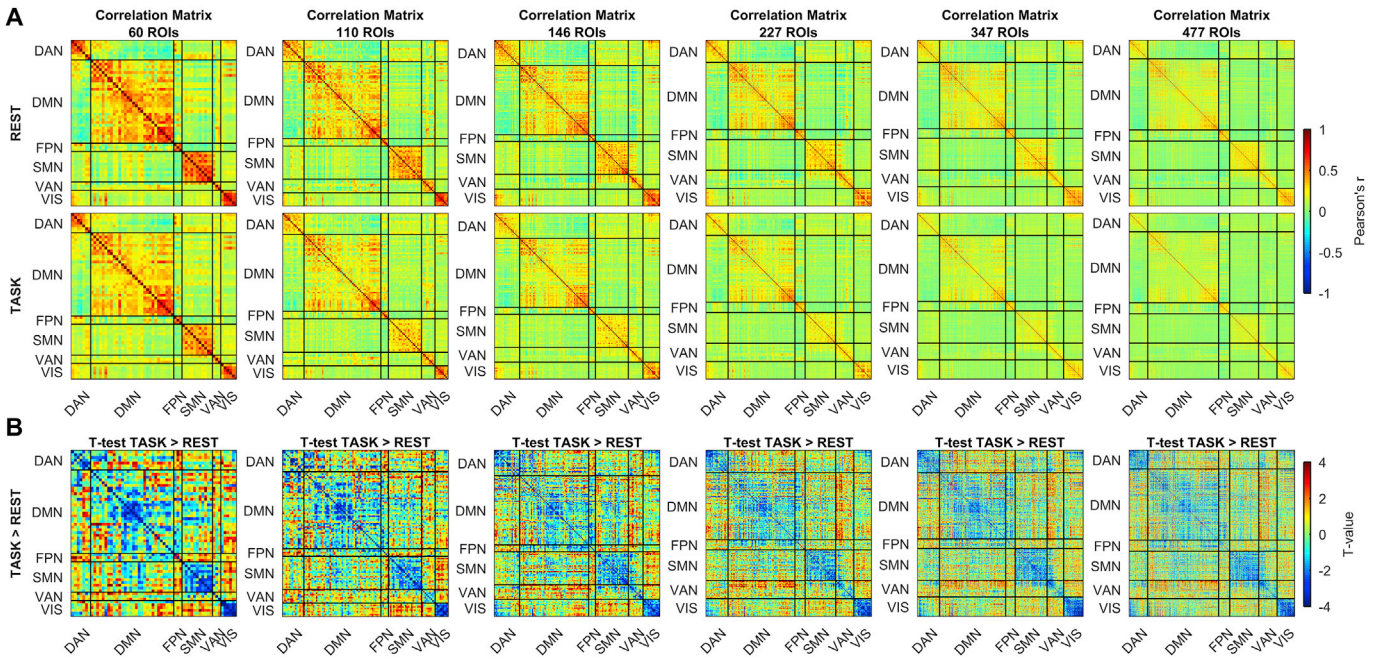

Fig. 5. Multi-scale assessment of task-associated changes in FC. Columns present the analysis of correlation matrices at different parcellation sizes, from 60 to 477 ROIs. **(A)** shows the group-level matrices obtained averaging separately the rest and task-related correlation matrices. **(B)** shows results of the unthresholded paired *t*-test, task > rest.

(Supplementary figure 4).

Visual examination of the plots in Fig. 7, as well as the results of general linear modelling of task vs rest connectivity across ROIs (Table 1) indicated that the swap from rest to task is associated with two effects: a rigid, whole-brain switch to higher values of connectivity (β_0 in Table 1), and a slope linking connectivity during task and at rest that is positive but less than unitary (β_1 in Table 1). In other words, the task-associated change of connectivity is a decreasing function of connectivity at rest (eq. (2), with $0<\beta_1<1$). The multi-scale patterns of connectivity changes shown in Fig. 5B are largely explained by this effect, insofar connectivity between ROIs in the same network is generally high (Fig. 5A), and thus the effect of $FC_R{}^*\beta_1$ is large and overcomes the effect of β_0, resulting in a decrease of connectivity, while the opposite is true for connectivity between ROIs in different networks. Overall, on average in all networks and subjects, the variance of ΔFC is dominated by the linear term in eq. (2) ($R^2 = 0.36$), while the constant term accounts for about one sixth of the linear term variance ($R^2 = 0.06$).

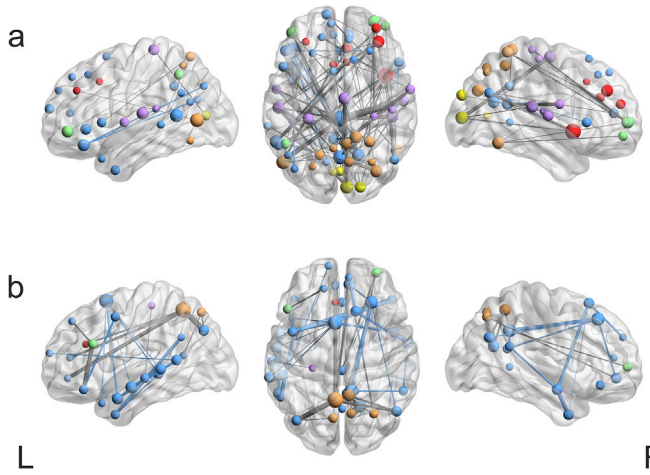

Fig. 6. Spatial representation of significant FC changes for the 110-ROIs parcellation scheme. Significant task-associated changes in FC were assessed via paired *t*-test (thresholded at *p*-FDR < 0.05) and visualized in BrainNet Viewer (Xia et al., 2013). Colour code represents ICA derived networks as in Fig. 1, line thickness represents significance of connectivity changes and sphere radius represents the degree centrality (number of significant edges associated with a given node). (**a**) Representation of the inter-networks connections increasing during task compared to rest condition. (**b**) Representation of the inter-networks connections decreasing during task compared to rest condition.

3.5. Behavioural relevance of functional connectivity findings

The most striking confirmation of the physiological relevance of the slope of FC_T vs FC_R comes from the analysis of behavioural correlates of the connectivity changes. Subjects' accuracy was significantly and positively correlated with connectivity between several networks both at rest and during task (Fig. 8A). The effect at rest was strong for connectivity between DMN and VAN/DAN, but was also significant for connections with VIS, and within SMN. During task, the correlation was very high and significant between DMN on one side and VAN and SMN on the other. In spite of this complex pattern of correlations, the association between subjects' accuracy and change (i.e. difference) of connectivity between task and rest tended to be weakly negative and did not reach significance for any couple of networks. However, we found a strong inverse correlation between subject's accuracy and β_1 of VAN-DAN and VAN-DMN connectivity, as well as β_1 of connectivity within DMN (Fig. 8B, model parameters are estimated from the 110-parcellation scheme). In other words, the lower the slope of FC_T vs FC_R, the higher the accuracy. Subject's accuracy was not correlated to β_0 (*p*-FDR > 0.9). Finally, the correlation matrices between subject's accuracy and model parameters (i.e., β_1 and β_0) were highly reproducible across all the investigated scales as demonstrated by significant Kendall coefficients of concordance (W) among correlation matrices ($W = 0.81$, $p < 10^{-11}$ for β_1 and $W = 0.79$, $p < 10^{-10}$ for β_0).

4. Discussion

Spontaneous low-frequency BOLD fluctuations characterize the physiological brain activity both at rest and during task execution.

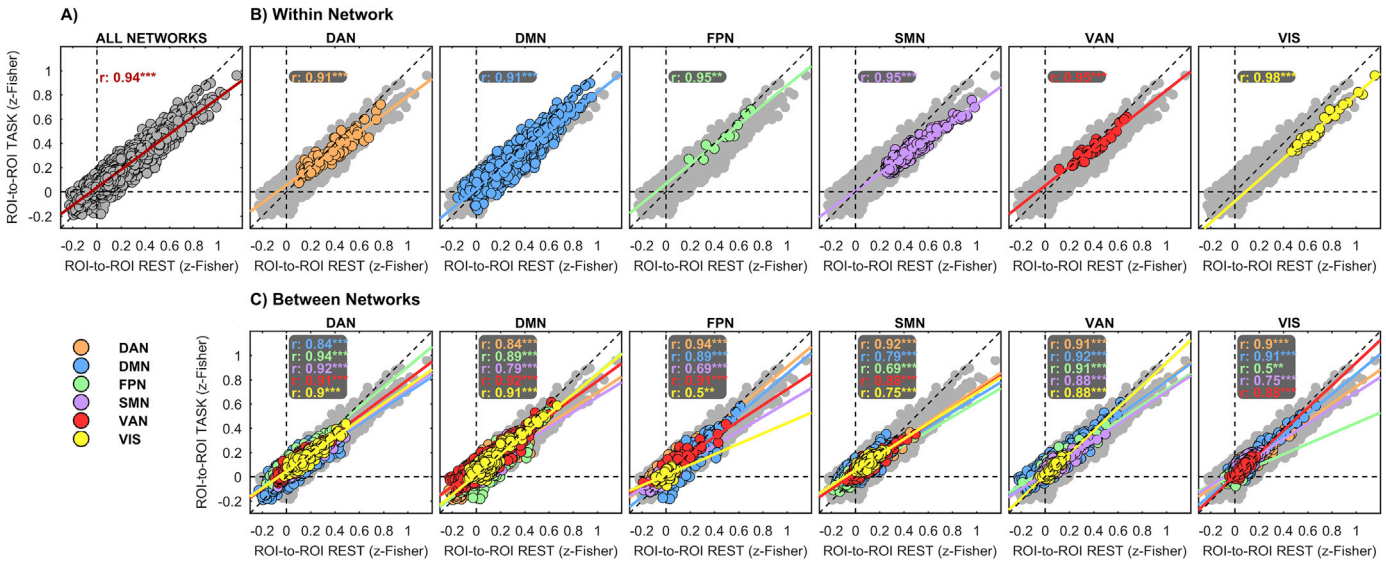

Fig. 7. ROI-based task vs rest FC relationship. Functional connectivity at rest was highly correlated to functional connectivity at task. Correlations were computed between the rest and task group-level 110-ROIs matrices (**A**). The same correlation was computed separately for each set of ROIs belonging to a given ICA-derived network (**B, within-network plots**) and for each set of ROIs correlations belonging to a given couple of networks (**C, between-network plots**). Network membership is marked by different colours. In each plot, the fit of the linear model in eq. (1) is also plotted. As reference, color-coded ROIs correlations in (B) and (C) are plotted on top of all possible ROI correlations, marked in light-grey colour.

Indeed, when the brain is engaged in a cognitive activity, low-frequency fluctuations coexist with the task-related BOLD response. Despite their proved relevance, how they get modulated during a sustained stimulation, as well as the behavioural relevance of their modulation, is still matter of debate (Gonzalez-Castillo and Bandettini, 2017). We sought to characterize the task-associated modulation of low-frequency fluctuations by means of a multi-parametric and multi-scale approach, in order to define the spatial scale of connectivity changes.

Previous similar studies usually adopted conventional block-design paradigms including relatively short epochs to disentangle ongoing brain activity from task-evoked response, combined with regression techniques that heavily rely on a correct modelling of bulk BOLD response to task (e.g. see Gonzalez-Castillo and Bandettini, 2017; and references in Anticevic et al., 2012). Modelling the BOLD response in order to remove it as a confound is an open issue: for example, BOLD response is known to be non-linear with the stimulus duration (Miller et al., 2001; Vazquez and Noll, 1998; Yeşilyurt et al., 2008). We chose to employ a modest number of protracted steady-state epochs (5 min each) that can be treated separately, and where the relative weight of hemodynamic response transients is minimized. Moreover, epoch to epoch variability and slow drifts of bulk BOLD response to task are outside the passband of the filter. Albeit it is not clear how the brain response adapts to continuous stimulations (e.g. Simon and Buxton, 2015), long stimulation epochs have been exploited in a number of functional studies on humans (Bandettini et al., 1997; Howseman et al., 1998), and a stable metabolic response was reported (Mangia et al., 2006). Steady-state conditions were exploited as well for studies of functional connectivity conceptually similar to the present paper (Hampson et al., 2006; Newton et al., 2007, 2011). Recently, Kwon and colleagues showed that longer epochs result in better sensitivity to connectivity changes associated to task, ruling out a major role of vascular confounds (Kwon et al., 2017). The reported evidence suggests that our results are mainly determined by the connectivity arising from ongoing BOLD fluctuations rather than from focal response. However, these signals are very difficult to completely disentangle, and the presence of residual contaminations cannot be entirely ruled out.

4.1. Multi-scale connectivity modulations during sustained WM stimulation

We adopted a multi-parametric approach to study task-related modulations of spontaneous BOLD low-frequency fluctuations, and observed a complex pattern of adjustments during task. Modulations in the synchronization of low-frequency fluctuations were found in large part the cerebral cortex, including both DMN and task-related networks (sensorimotor, frontoparietal and attentional). During task, the internal synchronization of networks was generally reduced, as indicated by decreased within-network FC (Fig. 2). The task-associated decrease of correlation at full network scale was accompanied by increased functional segregation at voxel scale, as indicated by decreased ReHo (Fig. 4A). The two effects were indeed correlated (Fig. 4B), suggesting that a task-driven decrease of correlation within functionally homogeneous areas is a scale invariant feature of the brain function, as confirmed by multi-scale analysis, which showed reduced within-network connectivity during task for all parcellation schemes (Fig. 5). These results are in agreement with the findings reported by Hampson et al. (2004), who found a more spatially limited network during a motion detection task compared to resting state, suggesting that a smaller network engages specifically during a visual task. Similar findings were also reported by Fransson and colleagues (Fransson, 2006), who found reduced connectivity in the DAN during sustained tasks, and by Gordon et al. (2014), who reported a reduced connectivity within the temporoparietal network during a working memory task.

However, while we observed a systematic reduction of connectivity within networks, we also observed an increase of connectivity between networks during task execution (Fig. 3), which was also observed at different parcellation schemes (Fig. 5). Indeed, other works reported that some classes of tasks, including n-back working memory, tend to increase connectivity in a number of task-relevant networks (Hampson et al., 2002; Lowe et al., 2000; Newton et al., 2007, 2011), while contrasting findings were found in the DMN, that showed either an increase or a decrease of task-associated connectivity (Fransson, 2006; Gordon et al., 2014; Hampson et al., 2006; Newton et al., 2011).

The only network where changes of ReHo were uncorrelated to changes of FC was the VAN. Comparing Fig. 2 with Fig. 4, the effect seems related to a small task-related FC modulation when probed at

Table 1
General linear model results of task vs rest connectivity across networks. A linear model between functional connectivity at rest and task was tested according to equation $FC_T = \beta_1 FC_R + \beta_0$. The switch from rest to task is mainly explained by two effects: a rigid, whole-brain switch to higher values of connectivity (β_0) and a positive, but less than unitary, slope between connectivity at task and at rest (β_1). These two effects are broadly uncorrelated, but they showed inverse correlation in some networks, as indicated by correlation values between β_0 and β_1 highlighted in red. Significance is marked with asterisk: *** $p < 0.001$, ** $p < 0.01$, * $p < 0.05$, FDR corrected.

	DAN	DMN	FPN	SMN	VAN	VIS
DAN	$\beta_1 = 0.622 \pm 0.028$*** $\beta_0 = 0.095 \pm 0.016$*** $R = -0.557$*	0.549 ± 0.026*** 0.043 ± 0.011*** -0.294 29	0.666 ± 0.032*** 0.085 ± 0.013*** -0.316	0.546 ± 0.027*** 0.064 ± 0.012*** -0.289	0.575 ± 0.027*** 0.065 ± 0.012*** 0.129	0.557 ± 0.047*** 0.067 ± 0.014*** -0.594*
DMN	0.686 ± 0.025*** 0.055 ± 0.008*** -0.404		0.702 ± 0.023*** 0.024 ± 0.011* -0.508	0.446 ± 0.027*** 0.046 ± 0.007*** -0.292	0.625 ± 0.021*** 0.075 ± 0.012*** -0.656**	0.595 ± 0.038*** 0.040 ± 0.012** 0.061
FPN			0.704 ± 0.029*** 0.118 ± 0.031** -0.781***	0.392 ± 0.042*** 0.015 ± 0.009 -0.038	0.607 ± 0.023*** 0.073 ± 0.016*** -0.398	0.363 ± 0.069*** 0.010 ± 0.015 -0.383
SMN				0.607 ± 0.018*** 0.054 ± 0.015** -0.400	0.504 ± 0.032*** 0.047 ± 0.008*** -0.420	0.452 ± 0.042*** 0.078 ± 0.011*** 0.030
VAN					0.627 ± 0.027*** 0.114 ± 0.017*** -0.673**	0.541 ± 0.047*** 0.035 ± 0.014* -0.062
VIS						0.762 ± 0.034*** 0.000 ± 0.032 -0.862***

network scale. Inspection of Fig. 5 indicates that the cause is probably the relatively heterogeneous response within the ICA-derived VAN network. Indeed, anterior part of VAN, specifically the middle temporal gyrus, at highest parcellation schemes (from 146) showed a substantial increase of connectivity to DMN and a decrease of connectivity to SMN. The effect is much lower in the posterior section of VAN (see Fig. 5). The fact that the described behaviour disappears in presence of parcellation into larger ROIs may indicate that it is governed by phenomena that have a high spatial specificity, but it can be related also to the exclusion of an increased proportion of boundary areas between networks in presence of larger ROIs (see methods). Even in the context of an overall preserved topology (see below), these results indicate a possible task-driven dissociation within the VAN. Our study was not specifically aimed at identifying flexible areas (i.e., areas shifting between networks, e.g., Bray et al., 2015), nonetheless, some connectivity changes, involving (beyond VAN) nodes in FPN, DAN, DMN and sensorial areas, were especially conspicuous (Fig. 6).

The described changes of within-network FC were widespread (Fig. 2) and were significant both in DMN and in SMN, DAN, VIS, FPN and VAN, the latter group being broadly overlapped to the "task positive" network, as introduced by Fox et al. (2005). It should be noted that the stimulation was an attention-demanding task but included also auditory and visual cues with in addition a modest motor task for the feedback, and indeed the conventional functional response was pervasive as well (Supplementary Figure 2). ReHo changes were more consistent across the cortex. In contrast, previous studies have shown mainly localized ReHo enhancements during conventional motor task performance in humans (Lv et al., 2013; Zang et al., 2004) and in rodents (Goelman, 2004).

4.2. Task level effect

FC and ReHo showed a tendency to respond to task level, but this effect did not reach generalized statistical significance, thus all the subsequent results refer to the averaged effect of the two task levels. It should be noted, however, that the small effect of task level, when present, was coherent with the mean change, i.e., increase of task difficulty tended to further reduce functional connectivity and ReHo. Such trend is in agreement with Esposito et al. (2006) who reported a task level related increment of deactivation in DMN and in conceptual agreement with Newton et al. (2011) who, however, reported the opposite change of connectivity in response to a similar n-back task. Several fMRI studies showed that increasing WM load mainly results in a deeper involvement of the same networks, thus increasing the degree of either activation or deactivation, according to the brain area, without substantial pattern changes (Leung et al., 2004; Newton et al., 2011; Pyka et al., 2009), However, other studies reported that modulations of task load can effectively recruit new areas (Tomasi et al., 2007) or elicit internal differentiation within the involved areas (Gould et al., 2003). We were not able to find a consistent effect of task load, while the mean effect of task was very strong. This result can be related to the fact that FC and ReHo changes between epochs at different task level were much more similar to changes among rest epochs than to changes between task and rest (see Figs. 2–4). Ultimately, a higher sensitivity would be needed to confirm subtle effects of WM load.

4.3. Stability of topology

Despite the diffuse and massive changes of the connectivity strength at both local and large scale, and of the opposite sign of connectivity change within and between networks, the overall topology of cortical connectivity was surprisingly stable, in agreement with the suggestion that the architecture of functional connectivity at rest is the main determinant of functional networks during activation (Cole et al., 2014). This effect can be understood considering that ΔFC is a negative function of FC_R in the whole brain (Table 1), and the overall sign of ΔFC is mainly determined by FC_R (the linear term of eq. (2) explains 36% of ΔFC variance). The DMN did not show any specific tendency to disengage

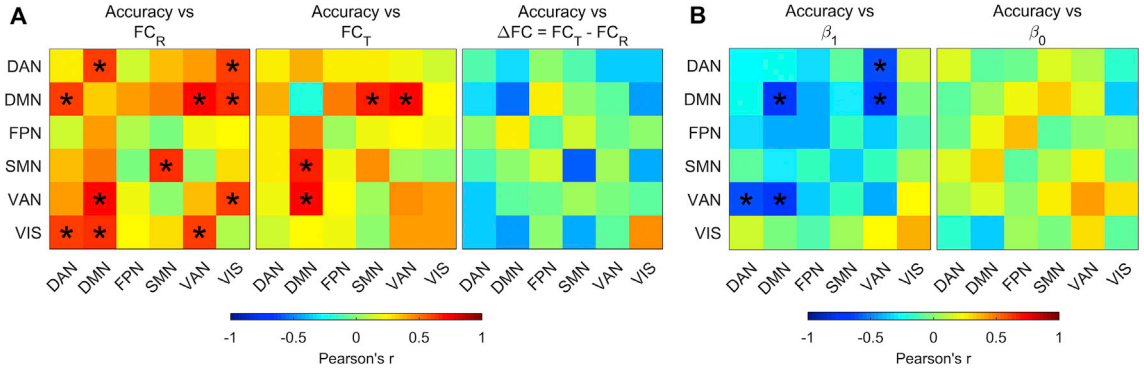

Fig. 8. The behavioural relevance of FC. A) Plots show correlations between working-memory subjects' accuracy and FC during resting epochs (left panel), during task epochs (middle panel) and with the relative change of connectivity, *ΔFC* (right panel). In all matrices, the main diagonal elements were replaced with correlations between accuracy and within-network FC. **B)** Plots show correlations between working-memory subjects' accuracy and β_1 (left) and β_0 (right) values. Performance did not show any significant correlation with β_0 (p-FDR > 0.9), while they showed strong negative correlations with β_1 for within DMN connectivity, VAN-DAN and VAN-DMN connectivity. In all plots significant correlations are marked with asterisks: * p-FDR < 0.05.

from other networks during task. In contrast, the DMN connectivity change in response to task was very similar to the connectivity change in other networks. Our observations can be explained by means of multi-scale synchronization. We propose that the change of functional connectivity during task is related to the overlapping of widespread, specialized processes at smaller scale, that increment specialization (i.e., decrease connectivity) in smaller areas, resulting in an average increase of heterogeneity, that causes a reduction of mean network connectivity. This hypothesis is supported by the fact that in 5 out of 6 networks, the change of network-scale connectivity was correlated with the change of ReHo (Fig. 4B). Notably, the only network where this correlation was not present is VAN, which showed a peculiar dissociation behaviour, as discussed above.

A possible confound suggested by our results is the massive change of between and within-network connectivity associated with task execution, a change that apparently involved all the considered networks, covering the majority of the cerebral cortex. In this context, techniques relying on averaging signals across the brain (global signal regression or related approaches, as used in Fransson, 2006; Hampson et al., 2002; Lowe et al., 2000; Newton et al., 2007; Newton et al., 2011) are supposed to rescale the connectivity changes between epochs, referring them to an average common behaviour in the same guise they mathematically mandate the emergence of spatial anticorrelations (Murphy et al., 2009). This can be especially true when considering that the change of FC within the DMN, which was the focus of all the mentioned works, had in our results the same sign, but a lower amplitude than in many other networks (Fig. 2). Whether referring regional task responses to the global brain signal is appropriate or not depends on the asked question and on the non-neural content of the latter (Murphy and Fox, 2017). In any case, the results that derive from a voxelwise measure, not affected by an arbitrary seed or threshold choice (the multi-scale analysis and ReHo), indicate that connectivity changes induced by task within the DMN are similar to and have the same sign of changes induced in task-positive networks.

4.4. Behavioural relevance of connectivity changes

Some of our connectivity findings were behavioural relevant at rest. Among the other network pairs, resting connectivity between DMN, DAN, VAN and VIS and between VAN and VIS was correlated to working memory accuracy, suggesting that large scale integration is a prerequisite for proper task performance. Behavioural relevance of connectivity at task was more focused, being confined to connectivity between DMN, SMN and VAN. The most conspicuous feature, however, was the lack of behavioural significance of connectivity change itself, together with a significant inverse correlation between the slope of connectivity at task vs connectivity at rest within the DMN and between VAN and DAN/DMN. Apparently, the bulk and widespread changes of connectivity we reported represent an overall effect that does not capture the behaviourally significant modulation of brain networks.

Indeed, the presence of a significant intercept in eq. (2) introduces a non-linear term in ΔFC, indicating that the change of connectivity is not related to connectivity at rest by a strictly linear relationship. This is especially important for studies focusing on connectivity changes. Indeed, from eq. (2), it is apparent that in presence of β_1 slightly under unity, connectivity change related to task (and in particular its sign) is determined by the interplay between the amplitude of positive β_0 and the small negative slope $\beta_1 - 1$, that implies a change of connectivity decreasing with increased connectivity at rest. In these conditions, the sign of the change is biased by the distribution of connectivity values at rest, with connections characterized by higher connectivity at rest more likely to end with a negative change.

Our results indicate that the behaviourally significant changes of connectivity are rather specific at network level. The relevant changes involve the connectivity between the ventral attention network on one side, and the dorsal attention network and the DMN on the other side, as well as the connectivity within the DMN. In all cases a reduced linear dependence of connectivity at task vs connectivity at rest (i.e. a lower slope, or a higher network reconfiguration) is related to an increased accuracy during an n-back task. This result is essentially opposite to the findings by Schultz and Cole (2016), reporting that in three different tasks an increased similarity between whole brain networks at rest and task (i.e. less reconfiguration during the task) predicts behavioural performance. This incongruence can be related to various reasons. The Schultz and Cole study involved a large number of subjects from the Human Connectome Project dataset, possibly highlighting some subtle whole-brain overall effect that was beyond detectability in our sample, while authors did not focus on network specific effects. This possibility is strengthened by the fact that authors found correlations also between network similarity and general intelligence, an effect likely to be unspecific to any given network. Moreover, the experimental approach was different, because Schultz and Cole exploited block designed short tasks, barely containing any power from the lowest part of the band of interest for BOLD low-frequency fluctuations, and relied on task regression, thus including a corresponding increased weight of hemodynamic transients (or rather, of discrepancy between subjective haemodynamic transients and the "canonical" response used in the modelling, see also Havlicek et al., 2017). This fact, compounded with the use of full-band analysis, biased the results towards a frequency band higher than the band we explored. If confirmed, this interpretation would strengthen the hypothesis that different bands of low-frequency fluctuations convey a substantially distinct information content (Betti et al., 2013; Tommasin et al., 2017). It should be noted that inclusion of higher frequencies in the analysis can have an impact on other aspects of connectivity changes as well, including the scale invariance we observed. Indeed, there is interaction between frequency of neurophysiological activity and spatial scale of its correlation structure (Hipp et al., 2012).

Our finding possibly help understanding while previous results had shown relationship between connectivity within DMN (and other networks) and performance, but generally failed to report a significant behavioural correlate of the connectivity change itself (Caceda et al., 2015; Hahamy et al., 2015; Hampson et al., 2006; Sadaghiani et al., 2015). In more general terms, the rather low specificity of the overall connectivity changes we observed, as well as the fact that it is influenced by a behaviourally irrelevant parameter β_0 and by connectivity at rest, questions the utility of the raw change of connectivity as metric in dynamic studies.

The fact that increases and decreases of connectivity coexist in a segregated and functionally meaningful distribution (Fig. 5) strongly speaks against possible artefactual origin of the effect. Indeed, resting-state fMRI confounds including vascular effect and head motion, are global in nature (Murphy et al., 2013), and do not follow network boundaries. Moreover, extensive preliminary testing showed that the results, and in particular the sign of the change of connectivity, is not impacted by different censoring approaches (see Methods), indicating that motion did not play a significant role in our results. The reported whole brain effect finds a physiological substrate in the large scale BOLD response to simple tasks (Gonzalez-Castillo et al., 2015 and references therein), and more directly in the widespread response to the task shown in Supplementary Figure 2.

Finally, our results indicate that without a proper normalization against reference connectivity values, the raw connectivity change may not be the most physiologically meaningful parameter. In this context, it is important to note that vascular reactivity is a powerful modulator of fMRI response, and it has been recently shown that vascular reactivity spatially modulates resting functional connectivity and amplitude of BOLD fluctuations (Golestani et al., 2016). Considering also the large range of intersubjective variability of vascular reactivity (Lipp et al., 2015), it would be interesting to assess the role of vascular reactivity in determining connectivity changes associated to task. Given that it cannot be excluded that effects like those we reported can be present not only between epochs, but also between subjects, the point deserves further investigation, also in consideration of the large and increasing use of

change of connectivity to study neurodegeneration.

4.5. Extrapolation to different domains

It is interesting to analyse to which extent our results can be extended to different cognitive domains and loads. The experiment was based on an auditory WM task that also involved the activity of other domains as highlighted above. The corresponding fMRI response spanned substantially the whole cortex (Supplementary figure 2).

Task-related decreases of within-network connectivity and increases of between-network connectivity have been repeatedly reported for several combinations of networks during attention (Kwon et al., 2017; Spadone et al., 2015), while various studies involving parametrically modulated WM tasks indicated a monotonic network modulation with cognitive load, e.g., in terms of change of connectivity within the DMN (Newton et al., 2007) or of integration between several large scale networks (Vatansever et al., 2015a). Cole and colleagues identified common patterns of connectivity at rest and during several task states, encompassing multiple domains, and reported crucially that there is a set of consistent network changes across all tasks (Cole et al., 2014). These findings taken together suggest that our results may generalize to different scenarios, however this hypothesis deserves further experimental investigation.

5. Conclusions

We conclude that the execution of a sustained working memory task, compounded with simple but coordinated motor and visual tasks, induces widespread changes of functional connectivity strength, with a spatial extent previously unreported. These changes showed the same trend at any probed connectivity range, and were dominated by connectivity at rest. The topology of network connectivity was largely unaffected by the task at whole cortex scale. Our results indicate that a multi-scale synchrony of the endogenous low-frequency BOLD fluctuations may represent a sustained global feature, whose strength modulations do not change the distributed features of the brain networks, and are possibly not relevant in absolute terms, being both linearly dependent on connectivity at rest and behaviourally irrelevant. On the contrary, our result supports the idea that controlling the connectivity changes for the value of connectivity at rest allows the identification of behaviourally relevant changes of brain connectivity, highlighting that an increased reconfiguration of involved networks (VAN, DAN and DMN) between rest and task foster increased task performance.

Contribution statement

ST and DM acquired and processed the data, prepared the figures and wrote the manuscript. MM acquired the data and performed the functional analysis. TG designed the study, programmed the stimulation and helped in the interpretation of the data. IEA and MF performed the experiment. MDN, RGW, SM, EM discussed the results and the manuscript and helped in the interpretation of the results. EM participated also in the study design. FG designed the study, interpreted the results and coordinated the research. All authors edited the text and approved the final version.

Acknowledgements

The present work was supported by the Italian Ministry for Education, University and Research (Ministero dell'Istruzione, dell'Università e della Ricerca, MIUR) under the grant "Progetto premiale NETFUN: NETwork FUNzionali cerebrali studiati con NMR" (Functional brain networks studied by NMR). Research reported in this publication was also supported by Regione Lazio, grant PAMINA (to F.G.) and by the National Institutes of Health, award number R01DK099137 (to S.M.). This project has received funding from the European Union's Horizon 2020 research and innovation programme under the Marie Skłodowska-Curie grant agreement No 691110 (MICROBRADAM). M.D.N. is supported by the European Union's Horizon 2020 research and innovation programme under the Marie Sklodowska-Curie grant agreement No 701635. The content is solely the responsibility of the authors and does not necessarily represent the official views of the funding bodies.

Appendix A. Supplementary data

Supplementary data related to this article can be found at https://doi.org/10.1016/j.neuroimage.2018.06.006.

References

Andersson, J.L., Hutton, C., Ashburner, J., Turner, R., Friston, K., 2001. Modeling geometric deformations in EPI time series. Neuroimage 13, 903–919.
Anticevic, A., Cole, M.W., Murray, J.D., Corlett, P.R., Wang, X.-J., Krystal, J.H., 2012. The role of default network deactivation in cognition and disease. Trends Cognit. Sci. 16, 584–592.
Bandettini, P.A., Kwong, K.K., Davis, T.L., Tootell, R.B., Wong, E.C., Fox, P.T., Belliveau, J.W., Weisskoff, R.M., Br, B.R.R., 1997. Characterization of cerebral blood oxygenation and flow changes during prolonged brain activation. Hum. Brain Mapp. 5, 93–109.
Beckmann, C.F., Smith, S.M., 2004. Probabilistic independent component analysis for functional magnetic resonance imaging. IEEE Trans. Med. Imag. 23, 137–152.
Behzadi, Y., Restom, K., Liau, J., Liu, T.T., 2007. A component based noise correction method (CompCor) for BOLD and perfusion based fMRI. Neuroimage 37, 90–101.
Betti, V., Della Penna, S., de Pasquale, F., Mantini, D., Marzetti, L., Romani, G.L., Corbetta, M., 2013. Natural scenes viewing alters the dynamics of functional connectivity in the human brain. Neuron 79, 782–797.
Braun, U., Schafer, A., Walter, H., Erk, S., Romanczuk-Seiferth, N., Haddad, L., Schweiger, J.I., Grimm, O., Heinz, A., Tost, H., Meyer-Lindenberg, A., Bassett, D.S., 2015. Dynamic reconfiguration of frontal brain networks during executive cognition in humans. Proc. Natl. Acad. Sci. U.S.A. 112, 11678–11683.
Bray, S., Arnold, A.E.G.F., Levy, R.M., Iaria, G., 2015. Spatial and temporal functional connectivity changes between resting and attentive states. Hum. Brain Mapp. 36, 549–565.
Caceda, R., James, A., Gutman, D.A., Kilts, C.D., 2015. Organization of intrinsic functional brain connectivity predicts decisions to reciprocate social behavior. Behav. Brain Res. 292, 478–483.
Calhoun, V.D., Kiehl, K.A., Pearlson, G.D., 2008. Modulation of temporally coherent brain networks estimated using ICA at rest and during cognitive tasks. Hum. Brain Mapp. 29, 828–838.
Cole, M.W., Bassett, D.S., Power, J.D., Braver, T.S., Petersen, S.E., 2014. Intrinsic and task-evoked network architectures of the human brain. Neuron 83, 238–251.
Cox, R.W., 1996. AFNI: software for analysis and visualization of functional magnetic resonance neuroimages. Comput. Biomed. Res. 29, 162–173.
Craddock, R.C., James, G.A., Holtzheimer, P.E., Hu, X.P.P., Mayberg, H.S., 2012. A whole brain fMRI atlas generated via spatially constrained spectral clustering. Hum. Brain Mapp. 33, 1914–1928.
Damoiseaux, J.S., Rombouts, S., Barkhof, F., Scheltens, P., Stam, C.J., Smith, S.M., Beckmann, C.F., 2006. Consistent resting-state networks across healthy subjects. Proc. Natl. Acad. Sci. U. S. A. 103, 13848–13853.
Elton, A., Gao, W., 2015a. Task-positive functional connectivity of the default mode network transcends task domain. J. Cognit. Neurosci. 27, 2369–2381.
Elton, A., Gao, W., 2015b. Task-related modulation of functional connectivity variability and its behavioral correlations. Hum. Brain Mapp. 36, 3260–3272.
Esposito, F., Bertolino, A., Scarabino, T., Latorre, V., Blasi, G., Popolizio, T., Tedeschi, G., Cirillo, S., Goebel, R., Salle, F.D., 2006. Independent component model of the default-mode brain function: assessing the impact of active thinking. Brain Res. Bull. 70, 263–269.
Fornito, A., Harrison, B.J., Zalesky, A., Simons, J.S., 2012. Competitive and cooperative dynamics of large-scale brain functional networks supporting recollection. Proc. Natl. Acad. Sci. U.S.A. 109, 12788–12793.
Fox, M.D., Snyder, A.Z., Vincent, J.L., Corbetta, M., Essen, D.C.V., Raichle, M.E., 2005. He human brain is intrinsically organized into dynamic, anticorrelated functional networks. Proc. Natl. Acad. Sci. U. S. A. 102, 9673–9678.
Fox, M.D., Snyder, A.Z., Vincent, J.L., Raichle, M.E., 2007. Intrinsic fluctuations within cortical systems account for intertrial variability in human behavior. Neuron 4, 171–184.
Fox, M.D., Snyder, A.Z., Zacks, J.M., Raichle, M.E., 2006. Coherent spontaneous activity accounts for trial-to-trial variability in human evoked brain responses. Nat. Neurosci. 9, 23–25.
Fransson, P., 2006. How default is the default mode of brain function? Further evidence from intrinsic BOLD signal fluctuations. Neuropsychologia 44, 2836–2846.
Gili, T., Cercignani, M., Serra, L., Perri, R., Giove, F., Maraviglia, B., Caltagirone, C., Bozzali, M., 2011. Regional brain atrophy and functional disconnection across Alzheimer's disease evolution. J. Neurol. Neurosurg. Psychiatry 82, 58–66.
Goelman, G., 2004. Radial correlation contrast–a functional connectivity MRI contrast to map changes in local neuronal communication. J. Neurol. Neurosurg. Psychiatry 23, 1432–1439.

Golestani, A.M., Kwinta, J.B., Strother, S.C., Khatamian, Y.B., Chen, J.J., 2016. The association between cerebrovascular reactivity and resting-state fMRI functional connectivity in healthy adults: The influence of basal carbon dioxide. Neuroimage 132, 301–313. https://doi.org/10.1016/j.neuroimage.2016.02.051.
Gonzalez-Castillo, J., Bandettini, P.A., 2017. Task-based dynamic functional connectivity: recent findings and open questions. Neuroimage.
Gonzalez-Castillo, J., Hoy, C.W., Handwerker, D.A., Roopchansingh, V., Inati, S.J., Saad, Z.S., Cox, R.W., Bandettini, P.A., 2015. Task dependence, tissue specificity, and spatial distribution of widespread activations in large single-subject functional MRI datasets at 7T. Cerebr. Cortex 25, 4667–4677.
Gordon, E.M., Breeden, A.L., Bean, S.E., Vaidya, C.J., 2014. Working memory–related changes in functional connectivity persist beyond task disengagement. Hum. Brain Mapp. 35, 1004–1017.
Gould, R.L., Brown, R.G., Owen, A.M., Ffytche, D.H., Howard, R.J., 2003. fMRI BOLD response to increasing task difficulty during successful paired associates learning. Neuroimage 20, 1006–1019.
Greicius, M., 2008. Resting-state functional connectivity in neuropsychiatric disorders. Curr. Opin. Neurol. 21, 424–430.
Hahamy, A., Sotiropoulos, S.N., Slater, D.H., Malach, R., Johansen-Berg, H., Makin, T.R., 2015. Normalisation of brain connectivity through compensatory behaviour, despite congenital hand absence. Elife 4 e04605.
Hampson, M., Driesen, N.R., Skudlarski, P., Gore, J.C., Constable, R.T., 2006. Brain connectivity related to working memory performance. J. Neurosci. 26, 13338–13343.
Hampson, M., Olson, I.R., Leung, H.C., Skudlarski, P., Gore, J.C., 2004. Changes in functional connectivity of human MT/V5 with visual motion input. Neuroreport 15, 1315–1319.
Hampson, M., Peterson, B.S., Skudlarski, P., Gatenby, J.C., Gore, J.C., 2002. Detection of functional connectivity using temporal correlations in MR images. Hum. Brain Mapp. 15, 247–262.
Havlicek, M., Roebroeck, A., Friston, K.J., Gardumi, A., Ivanov, D., Uludag, K., 2017. On the importance of modeling fMRI transients when estimating effective connectivity: a dynamic causal modeling study using ASL data. Neuroimage 155, 217–233.
Hipp, J.F., Hawellek, D.J., Corbetta, M., Siegel, M., Engel, A.K., 2012. Large-scale cortical correlation structure of spontaneous oscillatory activity. Nat. Neurosci. 15, 884–890.
Howseman, A.M., Porter, D.A., Hutton, C., Josephs, O., Turner, R., 1998. Blood oxygenation level dependent signal time courses during prolonged visual stimulation. Magn. Reson. Imaging 16, 1–11.
Huang, Z.R., Zhang, J.F., Longtin, A., Dumont, G., Duncan, N.W., Pokorny, J., Qin, P.M., Dai, R., Ferri, F., Weng, X.C., Northoff, G., 2017. Is there a nonadditive interaction between spontaneous and evoked Activity? Phase-Dependence and its relation to the temporal structure of scale-free brain activity. Cerebr. Cortex 27, 1037–1059.
Huijbers, W., Van Dijk, K.R.A., Boenniger, M.M., Stirnberg, R., Breteler, M.M.B., 2017. Less head motion during MRI under task than resting-state conditions. Neuroimage 147, 111–120.
Kriegeskorte, N., Simmons, W.K., Bellgowan, P.S.F., Baker, C.I., 2009. Circular analysis in systems neuroscience: the dangers of double dipping. Nat. Neurosci. 12, 535–540.
Kwon, S., Watanabe, M., Fischer, E., Bartels, A., 2017. Attention reorganizes connectivity across networks in a frequency specific manner. Neuroimage 144, 217–226.
Leech, R., Kamourieh, S., Beckmann, C.F., Sharp, D.J., 2011. Fractionating the default mode network: distinct contributions of the ventral and dorsal posterior cingulate cortex to cognitive control. J. Neurosci. 31, 3217–3224.
Leung, H.-C., Seelig, D., Gore, J.C., 2004. The effect of memory load on cortical activity in the spatial working memory circuit. Cognit. Affect Behav. Neurosci. 4, 553–563.
Lipp, I., Murphy, K., Caseras, X., Wise, R.G., 2015. Agreement and repeatability of vascular reactivity estimates based on a breath-hold task and a resting state scan. Neuroimage 113, 387–396.
Lowe, M.J., Dzemidzic, M., Lurito, J.T., Mathews, V.P., Phillips, M.D., 2000. Correlations in low-frequency BOLD fluctuations reflect cortico-cortical connections. Neuroimage 12, 582–587.
Lv, Y., Margulies, D.S., Villringer, A., Zang, Y.F., 2013. Effects of finger tapping frequency on regional homogeneity of sensorimotor cortex. PLoS One 8 e64115–e64115.
Mangia, S., Tkác, I., Gruetter, R., Moortele, P.F.V.D., Giove, F., Maraviglia, B., Uğurbil, K., 2006. Sensitivity of single-voxel 1H-MRS in investigating the metabolism of the activated human visual cortex at 7 T. Magn. Reson. Imaging 24, 343–348.
Mascali, D., DiNuzzo, M., Gili, T., Moraschi, M., Fratini, M., Maraviglia, B., Serra, L., Bozzali, M., Giove, F., 2015. Intrinsic patterns of coupling between correlation and amplitude of low-frequency fMRI fluctuations are disrupted in degenerative dementia mainly due to functional disconnection. PLoS One 10 e0120988–e0120988.
Mascali, D., DiNuzzo, M., Serra, L., Mangia, S., Maraviglia, B., Bozzali, M.F.,G., 2018. Disruption of semantic network in mild Alzheimer's disease revealed by resting-state fMRI. Neuroscience 371, 38–48.
Miller, K.L., Luh, W.M., Liu, T.T., Martinez, A., Obata, T., Wong, E.C., Frank, L.R., Buxton, R.B., 2001. Nonlinear temporal dynamics of the cerebral blood flow response. Hum. Brain Mapp. 13, 1–12.
Murphy, K., Birn, R.M., Bandettini, P.A., 2013. Resting-state fMRI confounds and cleanup. Neuroimage 80, 349–359.
Murphy, K., Birn, R.M., Handwerker, D.A., Jones, T.B., Bandettini, P.A., 2009. The impact of global signal regression on resting state correlations: are anti-correlated networks introduced? Neuroimage 44, 893–905.
Murphy, K., Fox, M.D., 2017. Towards a consensus regarding global signal regression for resting state functional connectivity MRI. Neuroimage 154, 169–173.
Newton, A.T., Morgan, V.L., Gore, J.C., 2007. Task demand modulation of steady-state functional connectivity to primary motor cortex. Hum. Brain Mapp. 28, 663–672.
Newton, A.T., Morgan, V.L., Rogers, B.P., Gore, J.C., 2011. Modulation of steady state functional connectivity in the default mode and working memory networks by cognitive load. Hum. Brain Mapp. 32, 1649–1659.
Piccoli, T., Valente, G., Linden, D.E.J., Re, M., Esposito, F., Sack, A.T., Di Salle, F., 2015. The default mode network and the working memory network are not anti-correlated during all phases of a working memory task. PLoS One 10.
Power, J.D., Barnes, K.A., Snyder, A.Z., Schlaggar, B.L., Petersen, S.E., 2012. Spurious but systematic correlations in functional connectivity MRI networks arise from subject motion (vol. 59, pg 2142, 2012). Neuroimage 63, 999–999.
Prodoehl, J., Burciu, R.G., Vaillancourt, D.E., 2014. Resting state functional magnetic resonance imaging in Parkinson's disease. Curr. Neurol. Neurosci. Rep. 14, 448–448.
Pyka, M., Beckmann, C.F., Schoning, S., Hauke, S., Heider, D., Kugel, H., Arolt, V., Konrad, C., 2009. Impact of working memory load on FMRI resting state pattern in subsequent resting phases. PLoS One 4, e7198.
Rogers, B.P., Morgan, V.L., Newton, A.T., Gore, J.C., 2007. Assessing functional connectivity in the human brain by FMRI. Magn. Reson. Imaging 25, 1347–1357.
Sadaghiani, S., Poline, J.B., Kleinschmidt, A., D'Esposito, M., 2015. Ongoing dynamics in large-scale functional connectivity predict perception. Proc. Natl. Acad. Sci. U. S. A. 11, 8463–8468.
Schultz, D.H., Cole, M.W., 2016. Higher intelligence is associated with less task-related brain network reconfiguration. J. Neurosci. 36, 8551–8561.
Simon, A.B., Buxton, R.B., 2015. Understanding the dynamic relationship between cerebral blood flow and the BOLD signal: implications for quantitative functional MRI. Neuroimage 116, 158–167.
Smith, S.M., Fox, P.T., Miller, K.L., Glahn, D.C., Fox, P.M., Mackay, C.E., Filippini, N., Watkins, K.E., Toro, R., Laird, A.R., Beckmann, C.F., 2009. Correspondence of the brain's functional architecture during activation and rest. Proc. Natl. Acad. Sci. U. S. A. 106, 13040–13045.
Spadone, S., Della Penna, S., Sestieri, C., Betti, V., Tosoni, A., Perrucci, M.G., Romani, G.L., Corbetta, M., 2015. Dynamic reorganization of human resting-state networks during visuospatial attention. Proc. Natl. Acad. Sci. U.S.A. 112, 8112–8117.
Spreng, R.N., Stevens, W.D., Chamberlain, J.P., Gilmore, A.W., Schacter, D.L., 2010. Default network activity, coupled with the frontoparietal control network, supports goal-directed cognition. Neuroimage 53, 303–317.
Tailby, C., Masterton, R.A.J., Huang, J.Y., Jackson, G.D., Abbott, D.F., 2015. Resting state functional connectivity changes induced by prior brain state are not network specific. Neuroimage 106, 428–440.
Tomasi, D., Chang, L., Caparelli, E.C., Ernst, T., 2007. Different activation patterns for working memory load and visual attention load. Brain Res. 1132, 158–165.
Tommasin, S., Mascali, D., Gili, T., Assan, I.E., Moraschi, M., Fratini, M., Wises, R.G., Macaluso, E., Mangia, S., Giove, F., 2017. Task-related modulations of BOLD low-frequency fluctuations within the default mode network. Frontiers in Physics 5.
Vatansever, D., Menon, D.K., Manktelow, A.E., Sahakian, B.J., Stamatakis, E.A., 2015a. Default mode dynamics for global functional integration. J. Neurosci.: Official J. Soc. Neurosci. 35, 15254–15262.
Vatansever, D., Menon, D.K., Manktelow, A.E., Sahakian, B.J., Stamatakis, E.A., 2015b. Default mode network connectivity during task execution. Neuroimage 122, 96–104.
Vazquez, A.L., Noll, D.C., 1998. Nonlinear aspects of the BOLD response functional MRI. Neuroimage 7, 108–118.
Whitfield-Gabrieli, S., Nieto-Castanon, A., 2012. Conn: a functional connectivity toolbox for correlated and anticorrelated brain networks. Brain Connect. 2, 125–141.
Xi-Nian Zuo, Ting, Xu, Lili Jiang Zhi, Yang, Xiao-Yan, Cao, Yong, He, Yu-Feng, Zang, Xavier Castellanos, F., Milhamf, M.P., 2013. Toward reliable characterization of functional homogeneity in the human brain: preprocessing, scan duration, imaging resolution and computational space. Neuroimage 65, 374–386.
Xia, M.R., Wang, J.H., He, Y., 2013. BrainNet viewer: a network visualization tool for human brain connectomics. PLoS One 8.
Yeo, B.T., Krienen, F.M., Sepulcre, J., Sabuncu, M.R., Lashkari, D., Hollinshead, M., Roffman, J.L., Smoller, J.W., Zoellei, L., Polimeni, J.R., Fischl, B., Liu, H., Buckner, R.L., 2011. The organization of the human cerebral cortex estimated by intrinsic functional connectivity. J. Neurophysiol. 106, 1125–1165.
Yeşilyurt, B., Uğurbil, K., Uludağ, K., 2008. Dynamics and nonlinearities of the BOLD response at very short stimulus durations. Magn. Reson. Imaging 26, 853–862.
Zang, Y., Jiang, T., Lu, Y., He, Y., Tian, L., 2004. Regional homogeneity approach to fMRI data analysis. Neuroimage 22, 394–400.